Measuring dark energy with expansion and growth

Louis Perenon [a,*], Matteo Martinelli [b], Roy Maartens [a,c,d], Stefano Camera [e,f,g,a], Chris Clarkson [h,a]

[a] *Department of Physics & Astronomy, University of the Western Cape, Cape Town 7535, South Africa*
[b] *INAF — Istituto Nazionale di Astrofisica, Osservatorio Astronomico di Roma, 00040 Monteporzio Catone, Italy*
[c] *Institute of Cosmology & Gravitation, University of Portsmouth, Portsmouth PO1 3FX, UK*
[d] *National Institute for Theoretical and Computational Sciences (NITheCS), Cape Town 7535, South Africa*
[e] *Dipartimento di Fisica, Università degli Studi di Torino, 10125 Torino, Italy*
[f] *INFN — Istituto Nazionale di Fisica Nucleare, Sezione di Torino, 10125 Torino, Italy*
[g] *INAF — Istituto Nazionale di Astrofisica, Osservatorio Astrofisico di Torino, 10025, Pino Torinese, Italy*
[h] *School of Physical & Chemical Sciences, Queen Mary University of London, London, E1 4NS, UK*

ARTICLE INFO

ABSTRACT

We combine cosmic chronometer and growth of structure data to derive the redshift evolution of the dark energy equation of state w, using a novel agnostic approach. The background and perturbation equations lead to two expressions for w, one purely background-based and the other relying also on the growth rate of large-scale structure. We compare the features and performance of the growth-based w to the background w, using Gaussian Processes for the reconstructions. We find that current data is not precise enough for robust reconstruction of the two forms of w. By using mock data expected from next-generation surveys, we show that the reconstructions will be robust enough and that the growth-based w will out-perform the background w. Furthermore, any disagreement between the two forms of w will provide a new test for deviations from the standard model of cosmology.

1. Introduction

Understanding dark energy remains a key problem in cosmology. A key quantity to trace the behaviour of dark energy is its equation of state $w(z) = \bar{p}_{de}(z)/\bar{\rho}_{de}(z)$, the ratio of the (spatially averaged) pressure and energy density. Deriving w is typically done using observations which infer background quantities such as the distance-redshift relation or the expansion rate as a function of redshift, $H(z)$. Then w can be estimated using a simple parametrisation or via non-parametric approaches (see e.g. [1–3] for reviews). A key problem in this approach is that whatever data is used, it needs to be differentiated in some way. In the case of distance data, such as from type Ia supernovae, two derivatives are required, greatly enhancing the error on $w(z)$ and increasing the sensitivity to the reconstruction approach that is used. While direct measurements of $H(z)$ only require one derivative to be taken, the observations themselves are much more sparse, e.g. from cosmic chronometers, or require extra assumptions, e.g. from baryon acoustic oscillations (BAO).

It is therefore important to access $w(z)$ in as many agnostic ways as possible. Here we present a new approach to direct reconstructions of $w(z)$ by including measurements of the growth rate $f(z)$. We show that in principle $w(z)$ can be found if we know $f(z)$ and $f'(z)$, together with $H(z)$ (and a prior on $\Omega_{m,0}$). Smoothing the measurements of these functions can give a direct measurement of $w(z)$. We do this smoothing using Gaussian Processes (GP), which has been shown to be particularly stable for taking derivatives of raw data [4,5]. This approach gives a new method for probing dark energy and gravity. In addition, it provides an important consistency test: if the growth-based w disagrees with the purely background w, this would signal a breakdown of the simple effective fluid model of dark energy (including quintessence models). The mismatch would be indicative of a clustering or interacting form of dark energy — or of a modification of general relativity.

The paper is organised as follows. We show in Section 2 how the dark energy equation of state can be obtained from background data only and derive how growth of structure data can be brought into play. In Section 3, we compare the predictions of the equations of state using current data, while in Section 4 we analyse their performances using forecasts on mock data and present the diagnostic which arises from comparing the background and growth equations of state. We summarise our findings in Section 5.

* Corresponding author.
  E-mail address: perenon.louis@yahoo.fr (L. Perenon).

2. Dark energy equation of state

Here we present two different methods to reconstruct $w(z)$ directly from data. The first is well known, and uses data that measures the background Hubble rate. The second is new and uses the time evolution of the growth rate.

The standard simple model of dynamical dark energy is defined by its equation of state $w(z)$. The dark energy is assumed to be non-interacting, so that it obeys energy conservation: $\dot{\bar{\rho}}_{de} + 3(1+w)H\,\bar{\rho}_{de} = 0$ (see e.g. [6] on interacting dark energy). It is assumed to be non-clustering on observable scales, which entails an implicit assumption that its speed of sound is close to 1 (see e.g. [7,8] on clustering dark energy).

The evolution of the Hubble rate is given in general relativity on a spatially flat background by

$$\frac{d\ln H}{d\ln(1+z)} \equiv -\frac{\dot{H}}{H^2} = \frac{3}{2} + \frac{3}{2}\,(1-\Omega_m)\,w\,, \tag{1}$$

$$\Omega_m(z) = \Omega_{m,0}\,H_0^2\,\frac{(1+z)^3}{H^2(z)}\,. \tag{2}$$

We can then reconstruct the equation of state using Eq. (1):

$$w_{bg} = \frac{1}{1-\Omega_m}\left[\frac{2}{3}\frac{d\ln H}{d\ln(1+z)} - 1\right], \tag{3}$$

where the subscript 'bg' indicates that this reconstruction involves only background quantities, i.e. $H(z)$, $dH(z)/dz$ and $\Omega_{m,0}$.

However, it also is possible to infer the equation of state from observations of cosmological perturbations. For example, redshift-space distortions (RSD) in galaxy correlations aim to measure the linear growth rate f of large-scale structure, a powerful probe of gravity. For standard models of dark energy in general relativity, at late times the linear growth factor D is scale-independent, if we neglect the effects of massive neutrinos. In this case, the linear matter density contrast is separable: $\delta_m(z, \boldsymbol{k}) = D(z)\,\delta_m(0, \boldsymbol{k})$. It then follows that the growth rate is scale independent:

$$f \equiv -\frac{\partial\ln\delta_m}{\partial\ln(1+z)} = -\frac{d\ln D}{d\ln(1+z)}\,. \tag{4}$$

Massive neutrinos introduce suppression and scale dependence in the linear power spectrum, but these effects are significantly smaller for the linear growth rate f [9]. Current constraints on the total mass of neutrinos are $M_\nu < 90$ meV at 95% confidence level (CL) [10]. In this mass range, the scale-dependent suppression of f is at sub-percent level on linear scales [11].

The perturbed conservation equations and the Poisson equation imply that

$$\ddot{\delta}_m + 2H\dot{\delta}_m - \frac{3}{2}\,\Omega_m H^2\,\delta_m = 0\,. \tag{5}$$

By Eq. (4), using $dz = -(1+z)H\,dt$, we have $\dot{\delta}_m = Hf\,\delta_m$ and $\ddot{\delta}_m = [(Hf)^{\cdot} + (Hf)^2]\,\delta_m$. Then Eq. (5) can be rewritten as an evolution equation for the growth rate:

$$\frac{d\ln f}{d\ln(1+z)} = f + 2 - \frac{d\ln H}{d\ln(1+z)} - \frac{3\Omega_m}{2f} \tag{6}$$

$$= f + \frac{1}{2} + \frac{3}{2}\,(\Omega_m - 1)\,w - \frac{3\,\Omega_m}{2f}\,.$$

Here the first line follows directly from Eq. (5) and the second line uses Eq. (1).

The second line in Eq. (6), which applies in standard dark energy models, implies that we can reconstruct $w(z)$ in a new way that incorporates structure formation and not only background information:

$$w_{gr} = \frac{1}{1-\Omega_m}\left\{\frac{2}{3}\left[f - \frac{d\ln f}{d\ln(1+z)}\right] - \frac{\Omega_m}{f} + \frac{1}{3}\right\}\,. \tag{7}$$

The subscript 'gr' indicates that we use growth data $f(z)$ and $df(z)/dz$, as well as background data — i.e. $H(z)$ data and a prior on $\Omega_{m,0}$. This gives a new method to extract the dark energy equation of state. Note that the concept of splitting key cosmological quantities into their background and perturbation or growth counter parts is not novel. More model-dependent methods have been considered in the past [12–17].

In our approach, by considering data on H, we can employ GP to reconstruct the evolution of H and then deduce dH/dz and Ω_m, given a value of $\Omega_{m,0}$. Then w_{bg} can be fully determined. Considering data on f and its GP reconstruction in addition, w_{gr} can be fully determined also. Then determining consistency between these gives a new diagnostic of dark energy and gravity, which we explore for present and upcoming experiments.

3. Reconstructions with current data

We use the 'Humble Code for Gaussian Processes' that we have made publicly available.[1] This code is able to compute automatically any combinations of kernels and their derivatives since it uses the python package SymPy. The first step to obtain the dark energy equations of state is to reconstruct the functions H and f with GP. We probe how robust the reconstructions are by looking at dependence on priors and assumptions, in order ensure that our conclusions are as agnostic as possible. Robustness tends to apply when the data is numerous and precise, an assumption that might not apply to current data.

For $H(z)$, we use cosmic chronometer (CC) data, via the compilation in Appendix A of [18]. We choose not to use the BAO data here, since they are less model-independent, requiring a prior on the sound horizon at recombination in order to be converted into measurements of $H(z)$. The $f(z)$ data are from [19], a compilation obtained from different tracers. This compilation contains only uncorrelated data and direct measurements of $f(z)$. We restrict all datasets to $z \leq 1$ in order to consider only the redshift range where data on both f and H are the most available.

As a first step, we explore the dependency of our results on the choice of priors for the means of the reconstructed functions. We choose not to enforce any mean prior on H and f. However, we also considered the case where predictions on these functions inferred from Planck data (within the ΛCDM model) are used as mean priors. We find that this produces negligible differences with the null prior case.

Secondly, we examine how the choice of GP kernel impacts the reconstructions. Since H and f are smooth functions of z, we use simple stationary kernels, comparing 3 kernels to cover the possible evolution of the data (see [20] for details of these kernels):

1. SE (squared exponential) is one of the most commonly used in cosmology as it is simple and predicts the smoothest evolution generally;
2. Mat32 (Matern 3/2) can capture the sharpest variations of the Matern class and is best able to capture noisy data;
3. RQ (rational quadratic) can be seen as an infinite sum of SE kernels with different correlation lengths, and an extra hyperparameter.

We optimise a GP for each kernel choice, for both H and f, ensuring that the allowed ranges on kernel hyperparameters are always chosen large enough to yield no effect. We take $[10^{-5},\ 10^5]$ for each hyperparameter. The results are displayed in Fig. 1. The ΛCDM model that we use is from CMB+BAO data (the last column of Table 2 in [21]). It is recovered within the 95% confidence regions of all the reconstructions, but some differences

---

[1] https://github.com/louisperenon/HCGP
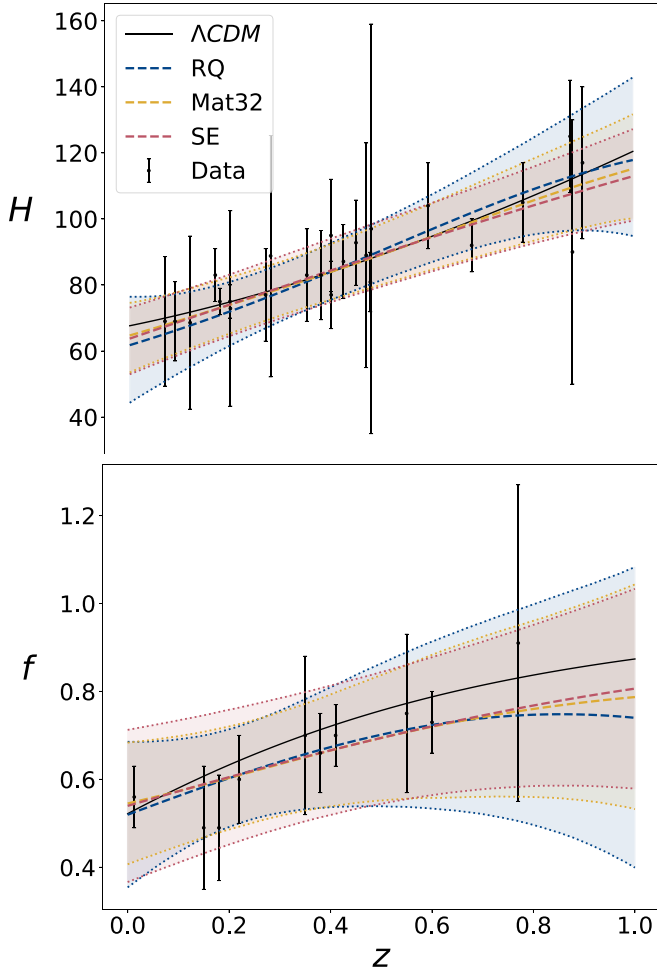
Fig. 1. Optimised reconstruction of H (top) and f (bottom) using 3 GP kernels. Means are dashed lines, shaded areas between dotted lines are 95% CL. ΛCDM is the solid black line.

are evident. The RQ kernel tends to yield the largest errors at the extremes of the data range, while Mat32 gives the smallest errors where the data clusters.

The data lacks constraining power. The fact that these three kernels yield different results overall is a hint that the quality of the current data is still too poor to produce more robust reconstructions. By contrast, reconstructions with future galaxy survey data do not suffer from this, see e.g. [22], and we will exploit this in Section 4.

Another key ingredient in the predictions of w_{bg} and w_{gr} is Ω_{m}, given in Eq. (2). It must be computed through the Monte Carlo realisation of two quantities, one from the GP on $H(z)$ and one from $\Omega_{\text{m,0}}$. While the possible realisations of $H(z)$ are entirely dictated by the CC data and the assumptions on the GP, the choice of $\Omega_{\text{m,0}}$ brings in an extra layer of prior knowledge that we need to examine. To illustrate how different values of $\Omega_{\text{m,0}}$ can impact the predictions, we use a Mat32 kernel for f and H and consider 3 different priors:

1. the Planck CMB+BAO constraint of Table 2 in [21], $\Omega_{\text{m,0}} = 0.3111 \pm 0.0056$;
2. the KiDS-DR3 constraint from AMICO galaxy clusters [23], $\Omega_{\text{m,0}} = 0.24^{+0.03}_{-0.04}$;
3. the DES Y3 constraint from weak lensing and galaxy clusters [24], $\Omega_{\text{m,0}} = 0.339^{+0.032}_{-0.031}$.
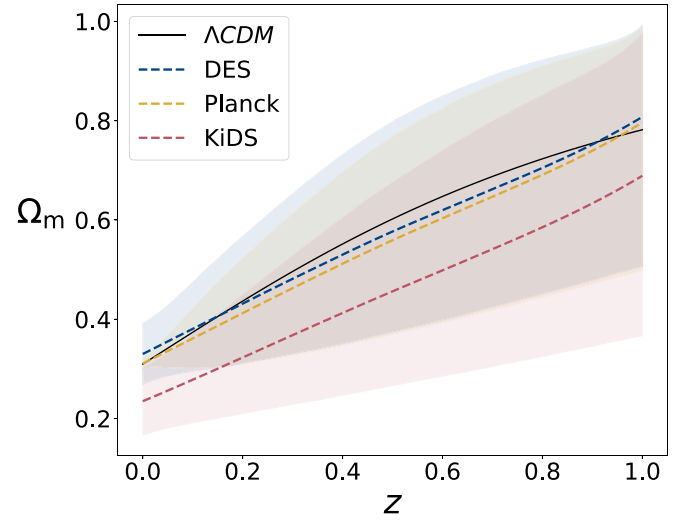
Fig. 2. Matter density $\Omega_{\text{m}}(z)$ from GP reconstruction of $H(z)$, with Mat32 kernel and 3 choices of prior on $\Omega_{\text{m,0}}$: DES Y3 (weak lensing and galaxy clusters); Planck CMB+BAO; KiDS-DR3 (AMICO galaxy clusters). Means are dashed lines, shaded areas are 95% CL.
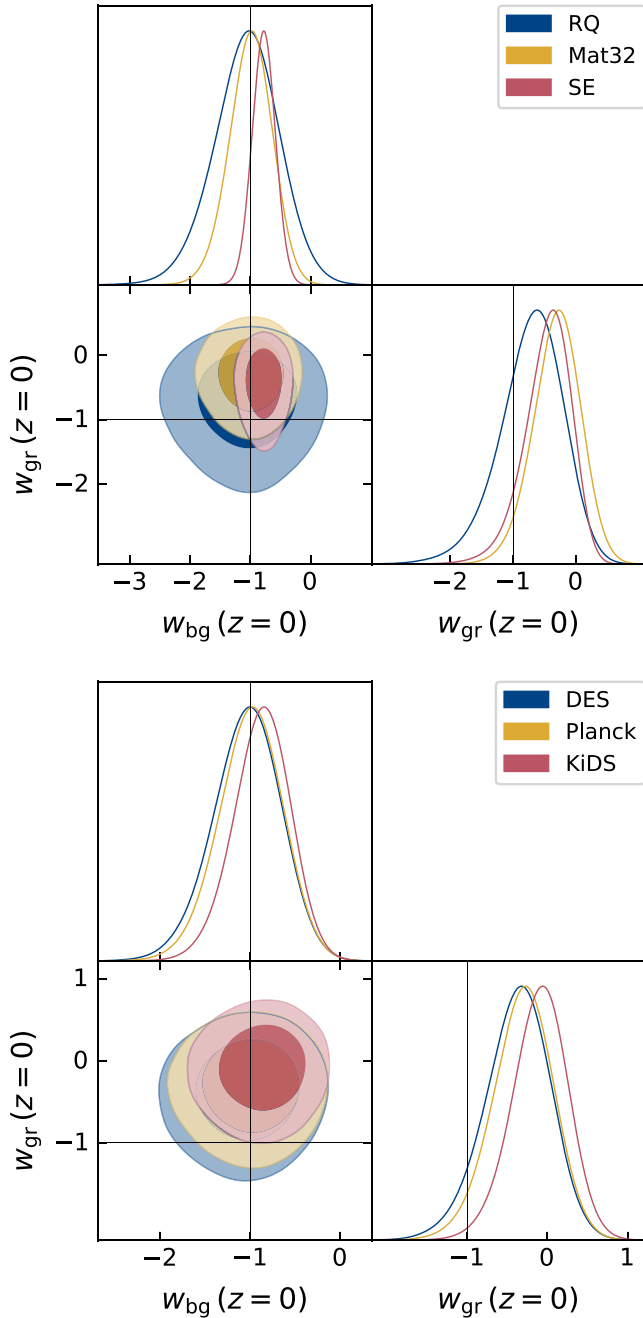
The results on the predictions of $\Omega_{\text{m}}(z)$ are shown in Fig. 2. The choice of prior on $\Omega_{\text{m,0}}$ is a key factor in the precision on $\Omega_{\text{m}}(z)$ at small redshifts, as expected. As redshift increases, uncertainties from the different prior choices becomes similar. Indeed, the error on $\Omega_{\text{m}}(z)$ becomes dominated by the uncertainty on $H(z)$.

Furthermore, there is an important caveat to consider in the prediction of $\Omega_{\text{m}}(z)$. Given our assumption of a spatially flat Universe, used to obtain Eqs. (3) and (7), we have a theoretical prior $\Omega_{\text{m}}(z) < 1$. Violating this condition is unphysical and would lead to divergence in w due to the $1/(1 - \Omega_{\text{m}})$ factors. Given the precision of the reconstruction of H and the choice of prior on $\Omega_{\text{m,0}}$, some realisations are however likely to violate this condition, in particular at higher redshift when matter starts to dominate over dark energy. The more precise is the data, the less probable are such occurrences. Using the kernel that leads to the smallest errors, i.e. Mat32, we find that with currently available data, 47%, 18% and 57% of the realisations violate such a condition for the 3 choices of $\Omega_{\text{m,0}}$ prior. This effect is another indication that more precise data is desirable to produce more robust predictions.

For now, we choose to reject the realisations that do not satisfy $\Omega_{\text{m}}(z) < 1$. The effect of this choice artificially pushes the mean of the prediction of Ω_{m} to lower values relative to the standard model, as seen in Fig. 2.

To derive the evolution of w_{bg} and w_{gr}, we use a Monte Carlo procedure. With a GP mean and covariance for $f(z)$ and $H(z)$, we can derive the mean and covariance of their derivatives (see [4] for details). Supplementing this with a prior on $\Omega_{\text{m,0}}$, we derive predictions of $\Omega_{\text{m}}(z)$. We then randomly simulate realisations of each of these quantities and from these derive a prediction of $w(z)$ at each step, following Eqs. (3) and (7). Their distribution at $z = 0$ for the different choices of kernel and priors is given in Fig. 3. Note that the constraints we find on w_{bg} are in good agreement with the recent findings of [25] using the same data set but a different method.
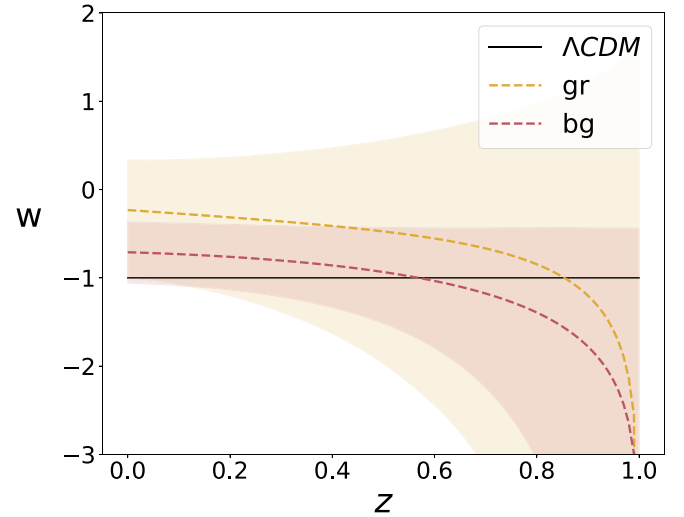
In the top panel, we use the Planck prior on $\Omega_{\text{m,0}}$ and compare the kernels. The RQ kernel leads to much larger errors, showing that the derivation of w can be very sensitive to kernel choice given the data that we use for the reconstruction. Note that the standard model ($w_{\text{bg}} = w_{\text{gr}} = -1$) is consistent within 95% CL for each kernel. Interestingly, there is a tendency for $w_{\text{gr}} > w_{\text{bg}}$.

Fig. 4. Derived predictions of w_{bg} and w_{gr} from Monte Carlo realisations of GP-generated f and H, with Mat32 kernel and KiDS prior on $\Omega_{m,0}$.

Fig. 3. Distribution of w_{bg} and w_{gr} at $z = 0$ from Monte Carlo realisations of GP-generated f and H and the derived Ω_{m}. *Top:* For Planck prior on $\Omega_{m,0}$ and different GP kernels (see Fig. 1). *Bottom:* For Mat32 kernel and different priors on $\Omega_{m,0}$ (see Fig. 2). Shading levels are 68% and 95% CL.

In addition, the SE and RQ kernels, which yield a w_{bg} centred around the standard model, produce a w_{gr} systematically larger than -1. This is a consequence of the fact that growth data has a slight preference for suppressed growth relative to the standard model [26–29]. As a result, the reconstructions of f tend to lie further below the standard model as can be seen in Fig. 1.

In the bottom panel, we fix the kernel of the reconstruction to Mat32, and compare the different priors on $\Omega_{m,0}$. The differences induced by changing prior are milder than those induced by changing kernel. We also observe that there is not a one to one correspondence between the error on $\Omega_{m,0}$ and that on $w(0)$. For example, the tightest prior on $\Omega_{m,0}$ is from Planck, and it does not

lead to the smallest error. It is in fact the error on the derivative of H which plays a key role. This is another example showing that the details of the GP reconstructions strongly affect the derivation of w and hence the choice of kernel is more important than the choice of $\Omega_{m,0}$ prior.

We observe a systematic increase of $w(0)$ when $\Omega_{m,0}$ decreases, although the results are always compatible with each other. This arises since a decrease in $\Omega_{m,0}$ increases the factor $(1 - \Omega_{m,0})^{-1}$ in Eqs. (3) and (7). The increase is enhanced for $w_{gr}(0)$ by the term $-\Omega_{m,0}/f(0)$. Nevertheless, the tendency to have $w_{gr} > -1$ is present no matter what the choice of $\Omega_{m,0}$ prior is.

Using a Mat32 kernel and the KiDS prior on $\Omega_{m,0}$, we display the redshift evolution of w_{bg} and w_{gr} in Fig. 4. The downward trend of the means at higher redshifts is a result of the $\Omega_{m}(z) < 1$ prior. However, as expected we find that such a requirement does not affect the distribution of w at low redshifts.

Although the reconstructed w_{bg} and w_{gr} are compatible with the standard model within 2σ, the tendency of the perturbation data to prefer a lower growth rate than in the standard model leads to hints for w_{gr} different from w_{bg}, with $w_{gr} > -1$. This could be a signal of deviations from the standard model. However, the precision and number of current data is too poor to make robust claims. The predictions are too sensitive to the details of the reconstructions, i.e. the GP kernels and the prior on $\Omega_{m,0}$. The analysis we developed here should become much more stringent with future data.

4. Forecasts with future surveys

In this section we estimate the precision that could be achieved by future surveys on the w derivations. We also analyse how effective this can be as a test of the standard model.

4.1. Reconstructing w_{bg} and w_{gr}

Instead of choosing specific surveys, we simply assume nominal surveys that deliver percent-level precision on H and f at low z, with errors growing as z increases. We create mock datasets for $f(z)$ and $H(z)$ with ΛCDM as fiducial. This gives predicted values at 11 redshifts uniformly distributed between redshift 0 and 1.

For f, we assume the errors start at 1% and grow as $(1 + z)$. For the cosmic chronometer data on H we use the prescription
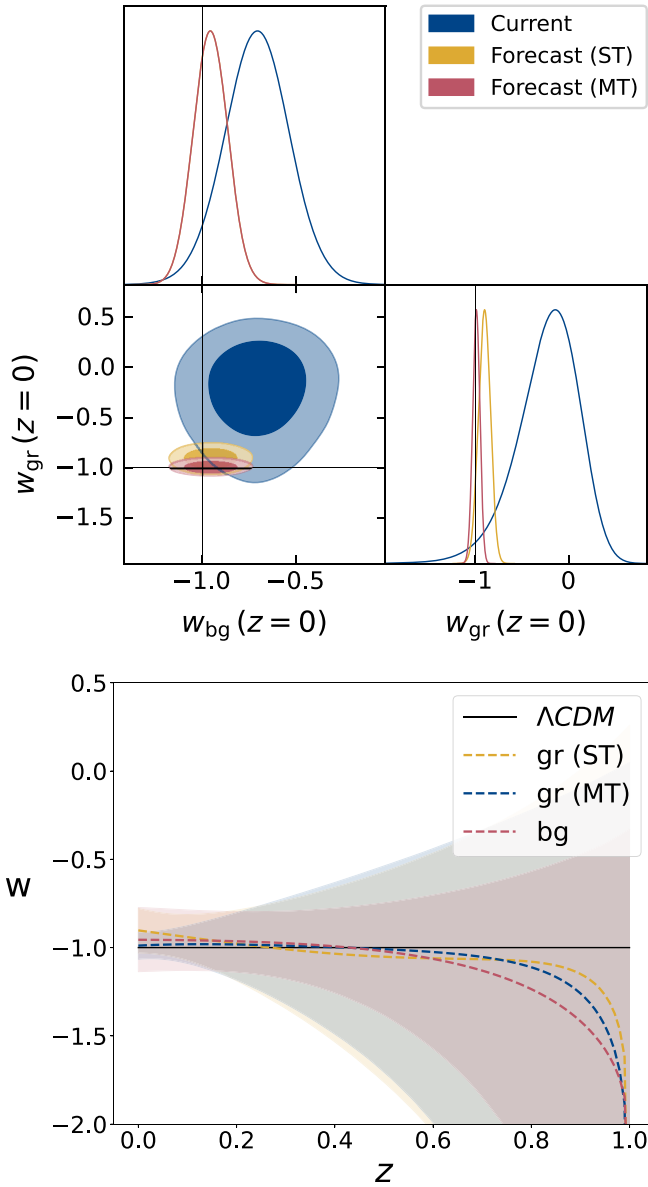
Fig. 5. Predictions of w_{bg} and w_{gr} from Monte Carlo procedure based on single- and multi-task GP reconstructions of f and H with mock future data. *Top:* Distributions at $z = 0$, compared to current data (as in Fig. 4 bottom panel, with KiDS prior). *Bottom:* Redshift evolution of w_{bg} and w_{gr}.

of [30], where the error on the spectroscopic velocity increases linearly from 1% to 11% from the first to the last measurement. Then for f and H, we draw the mocks from multivariate Gaussian distributions with mean given by their fiducial prediction. The diagonal covariance matrix entries are their errors squared. We also choose a prior on $\Omega_{m,0}$ with 1% error, in line with the expected precision of future weak lensing surveys.

We find that this precision on the data yields GP reconstructions much less dependent on the choices of kernel and priors than for current data. The reconstructions are now completely driven by the data [22]. We therefore choose an SE kernel and a null mean prior, as in [22]. We find that only 2.7% of the reconstructions are rejected by the $\Omega_m(z) < 1$ condition. The reconstructions produced are now much more robust and unbiased, compared to those extracted from current data.

At this level of precision, the benefits of including growth data to reconstruct w become apparent. We comment first on the results at $z = 0$, shown in Fig. 5, top panel. Comparing the widths of the constraints, it is evident that the w_{bg} error which uses only future cosmic chronometer data is decreased by factor ~ 2 relative to current data. When including future growth data, the w_{gr} error decreases by more than a factor of 5. We obtain for the forecast using background data:

$$w_{bg}(0) = -0.956\,^{+0.183}_{-0.181} \qquad (95\%\,\text{CL}). \tag{8}$$

This is improved by 44% when adding the forecast growth data:

$$w_{gr}(0) = -0.903\,^{+0.125}_{-0.128} \qquad (95\%\,\text{CL}). \tag{9}$$

Upcoming surveys will not only improve measurements of the growth rate $f(z)$, but will also obtain precise estimate of the two related functions, $\sigma_8(z)$ and $(f\sigma_8)(z)$. Spectroscopic galaxy surveys will allow for precise measurements of $(f\sigma_8)(z)$, while combinations of galaxy–galaxy lensing with RSD [31–33] or combining matter power spectrum and bispectrum [34–38], will break the $f\sigma_8$ degeneracy and extract measurements of f and σ_8.

With these measurements in hand, one can avoid reconstructing only f by combining the information contained in the measurements of the three functions. This can be done by reconstructing simultaneously f, σ_8 and $f\sigma_8$ via the use of multi-task GP, which greatly improves the error on the prediction of each quantity [22]. Following the procedure of [22], we use mock data to forecast σ_8 and $f\sigma_8$, using the same prescriptions as we have for f, and thus reconstruct simultaneously the three functions. Using now this multi-task (MT) reconstruction of f in the derivation of w_{gr}, we obtain

$$w_{gr,MT}(0) = -0.989\,^{+0.076}_{-0.077} \qquad (95\%\,\text{CL}). \tag{10}$$

This yields a 67% improvement on the single-task (ST) prediction Eq. (9).

At higher redshifts the picture is quite different. The error on w increases with z, since the error on the forecast data does. However, Fig. 5 bottom panel shows that the error on w_{bg} is smaller than that on w_{gr} — since w_{gr} depends on Ω_m/f. As the error on Ω_m increases with z, it comes to dominate the overall error on w_{gr}. For the same reason, there is virtually no gain at larger redshifts made by considering a multi-task reconstruction, even though the precision of the reconstruction on f is improved at all redshifts relative to the single-task case.

In order to illustrate the previous findings further, we run a large number of realisations of w, assuming that $\Omega_m(z)$ is known perfectly, i.e. fixing it to the fiducial. The results are informative: the error on w_{bg} does not improve while that on w_{gr} does considerably and is smaller at almost all redshifts. Its multi-task version is a factor 2 more precise than the single-task case. This shows that the error on Ω_m is significantly more detrimental to the prediction of w_{gr}, due to the Ω_m/f term. At low redshifts, the error on w_{gr} is always lower than for w_{bg}. For w_{gr} to become a more competitive diagnostic at high z, more precise constraints on $\Omega_m(z)$ are required.

Reconstructions of w_{bg} and w_{gr} provide a test of dark energy and gravity. Fig. 6 illustrates the potential diagnostics of this probe, using mock data sets for two non-standard models:

• $w_0 w_a CDM$: A dynamical dark energy model with $w(z) = w_0 - w_a\,z/(1+z)$ [39,40], whose fiducial values are constrained by the combination of CMB, BAO, RSD and weak lensing (last column of Table 6 in [21]). Fig. 6 top panel shows predictions for w_{bg} and w_{gr}. These recover the fiducial trend well and the previous findings on precision apply. At lower z the multi-task error on w_{gr} is lower than the single-task error, which in turn is lower than the w_{bg} error. w_{bg} excludes the standard model at more than 95% CL and w_{gr} excludes it with much higher significance.
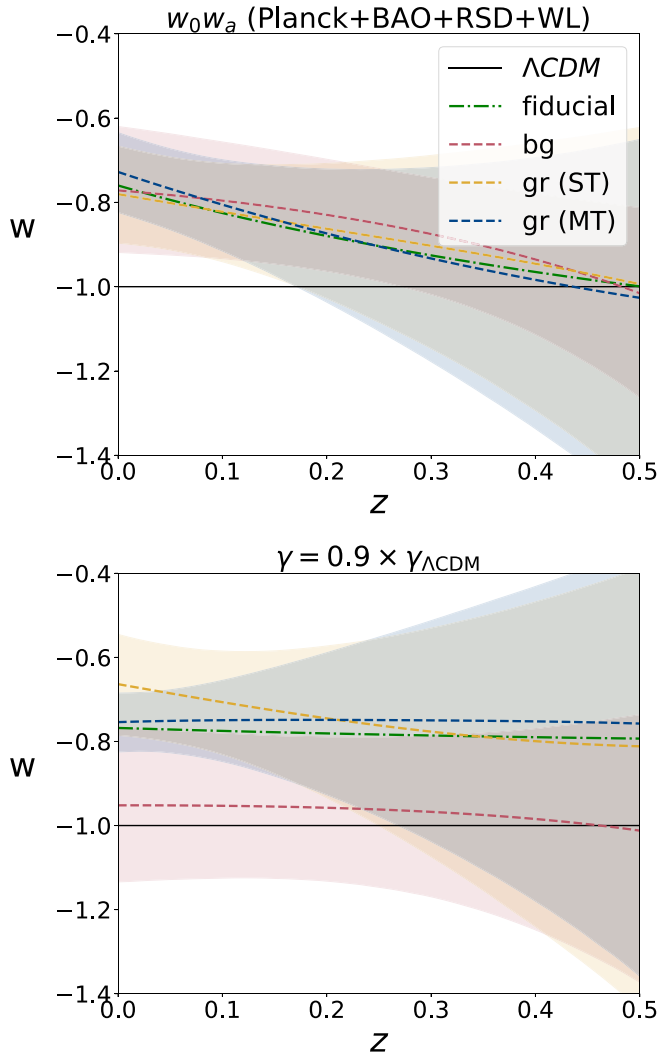
Fig. 6. As in Fig. 5 (bottom) but using mock data from non-ΛCDM models. *Top:* Predictions for $w_0 w_a$CDM as constrained by Planck [21]. *Bottom:* Predictions for a model with ΛCDM fiducial on H, while $f = \Omega_\mathrm{m}^\gamma$ with $\gamma \neq \gamma_{\lambda\mathrm{CDM}} = 0.55$.

- γCDM: A simplified modified gravity model which mimics a ΛCDM expansion rate but has different growth rate, where we use the parametrisation $f = \Omega_\mathrm{m}^\gamma$ [41,42]. We choose a -10% variation of the standard value $\gamma_{\Lambda\mathrm{CDM}} = 0.55$, and use the code MGCLASSII [43] to compute the fiducial predictions of f and σ_8. The bottom panel of Fig. 6 displays the w_bg and w_gr predictions. w_bg is fully consistent with the standard model, while w_gr (ST and MT) correctly follows the prediction of the modified fiducial. In fact, at low z the growth and background reconstructions exclude each other at almost 95% CL. This highlights that there is not only valuable phenomenological information to be gained from comparing w_bg and w_gr predictions with the standard model, but also from comparing them with one another.

4.2. A new diagnostic of gravity

We can turn the results in Fig. 6 into an effective diagnostic of gravity, based on the separation between pure-background reconstruction (H from cosmic chronometers in our analysis) and background + perturbation reconstruction (f in our case). By

comparing the reconstructions we can schematise the diagnostic as follows:

- If $w_\mathrm{bg} \neq -1$, this indicates a departure from standard ΛCDM. By Eq. (3), this could be caused by spatial curvature, dynamical dark energy or modified gravity (or a combination).
- If $w_\mathrm{gr} \neq -1$, there are 3 possible outcomes:
  * $w_\mathrm{bg} = w_\mathrm{gr} \neq -1$, so that background and growth are consistent, hinting at dynamical dark energy within General Relativity. Both reconstructions can be used to track down the redshift evolution of w, allowing us to test this.
  * $w_\mathrm{bg} \neq w_\mathrm{gr}$, so the standard ΛCDM again breaks down, but with inconsistency between background and growth. This could hint at clustering dark energy or modified gravity.
  * $w_\mathrm{bg} = -1$, so the background is compatible with standard ΛCDM but perturbations are incompatible. This could arise from scale-dependent growth in clustering dark energy or modified gravity models.

5. Conclusion

We propose a new way to reconstruct the equation of state of dark energy w by using the growth of large-scale structure. This approach is based on the evolution equation for the growth rate f. (Note that [44] use the same equation but for a different purpose, i.e. to reconstruct the evolution of Ω_m. For us, Ω_m is derived via reconstruction of H from data.)

There are two ways to reconstruct w: purely from background data (w_bg); adding perturbation data to background data (w_gr). We apply both approaches to current data, using cosmic chronometers and RSD. We find that the data is too noisy for the reconstructions of H and f to be robust enough under changes of GP kernels. Consequently, reconstructed w_bg and w_gr also show a dependency on the kernel. The method is also sensitive to an additional input: the choice of prior on $\Omega_{\mathrm{m},0}$. Nevertheless, we find the reconstructed w_bg and w_gr to be compatible with the standard model within 2σ. Slight tendencies are noticeable: suppressed growth relative to the standard model, w_gr different from w_bg, and $w_\mathrm{gr} > -1$. This could be a hint of deviations from the standard model that will be crucial to explore with future data.

Consequently, we explore the performance of our reconstruction technique with mock data from nominal future surveys. With enhanced precision the GP reconstructions are robust: we find that at $z = 0$ the error on w_bg is decreased by a factor of almost 2, while for w_gr the decrease is more than a factor of 5. This implies that the forecast error on w_gr is 44% more precise than that on w_bg at $z = 0$.

The precision on w_gr can be increased further by 67%, using a multi-task GP reconstruction of the data — where f, σ_8 and $f\sigma_8$ are reconstructed simultaneously. On the other hand, w_gr precision is more degraded than w_bg at higher redshifts by the uncertainties on the Ω_m reconstruction.

We also use forecast data with two non-standard models as fiducial, which are complementary: $w_0 w_a$CDM, where only the background deviates; γCDM where only the perturbations deviate ($f = \Omega_\mathrm{m}^\gamma$ and $\gamma \neq 0.55$). In both cases, we find that the reconstructions are precise enough to detect these deviations from the standard model. This allowed us to present a diagnostic to probe the phenomenology that can cause these deviations.

Summarising, our new method can provide some fresh insight into the dark sector of the Universe, based on a GP reconstruction

of the data. Our results hold within the range of validity of the GP method. Although this method is not completely model independent (see e.g. [22,45] for further discussion), it is 'agnostic', in the sense that it does not require a choice of a cosmological model. Our method is able to identify the contributions to w from background alone and from background + perturbations. In this sense, it is complementary and orthogonal to more standard, model-dependent data analyses techniques, with which it can be compared when future data becomes available.

CRediT authorship contribution statement

Louis Perenon: Software, Conceptualization, Methodology, Formal analysis, Investigation, Writing – original draft, Writing – review & editing, Visualization, Supervision, Project administration. **Matteo Martinelli:** Conceptualization, Methodology, Formal analysis, Investigation, Writing – original draft, Writing – review & editing, Visualization, Supervision, Project administration. **Roy Maartens:** Conceptualization, Methodology, Formal analysis, Investigation, Writing – original draft, Writing – review & editing, Visualization, Supervision, Project administration. **Stefano Camera:** Conceptualization, Methodology, Formal analysis, Investigation, Writing – original draft, Writing – review & editing, Visualization, Supervision, Project administration. **Chris Clarkson:** Conceptualization, Methodology, Formal analysis, Investigation, Writing – original draft, Writing – review & editing, Visualization, Supervision, Project administration.

Declaration of competing interest

The authors declare that they have no known competing financial interests or personal relationships that could have appeared to influence the work reported in this paper.

Acknowledgements

References

[1] V. Sahni, A. Starobinsky, Reconstructing dark energy, Internat. J. Modern Phys. D 15 (2006) 2105–2132, http://dx.doi.org/10.1142/S0218271806009704, arXiv:astro-ph/0610026.

[2] A. Silvestri, M. Trodden, Approaches to understanding cosmic acceleration, Rep. Progr. Phys. 72 (2009) 096901, http://dx.doi.org/10.1088/0034-4885/72/9/096901, arXiv:0904.0024.

[3] D. Huterer, D.L. Shafer, Dark energy two decades after: Observables, probes, consistency tests, Rep. Progr. Phys. 81 (1) (2018) 016901, http://dx.doi.org/10.1088/1361-6633/aa997e, arXiv:1709.01091.

[4] M. Seikel, C. Clarkson, M. Smith, Reconstruction of dark energy and expansion dynamics using Gaussian processes, J. Cosmol. Astropart. Phys. 06 (2012) 036, http://dx.doi.org/10.1088/1475-7516/2012/06/036, arXiv:1204.2832.

[5] M. Seikel, C. Clarkson, Optimising Gaussian processes for reconstructing dark energy dynamics from supernovae, 2013, arXiv:1311.6678.

[6] R. Kase, S. Tsujikawa, General formulation of cosmological perturbations in scalar-tensor dark energy coupled to dark matter, J. Cosmol. Astropart. Phys. 11 (2020) 032, http://dx.doi.org/10.1088/1475-7516/2020/11/032, arXiv:2005.13809.

[7] F. Hassani, J. Adamek, M. Kunz, Clustering dark energy imprints on cosmological observables of the gravitational field, Mon. Not. R. Astron. Soc. 500 (4) (2020) 4514–4529, http://dx.doi.org/10.1093/mnras/staa3589, arXiv:2007.04968.

[8] R.C. Batista, A short review on clustering dark energy, Universe 8 (1) (2021) 22, http://dx.doi.org/10.3390/universe8010022, arXiv:2204.12341.

[9] F. Villaescusa-Navarro, A. Banerjee, N. Dalal, E. Castorina, R. Scoccimarro, R. Angulo, D.N. Spergel, The imprint of neutrinos on clustering in redshift-space, Astrophys. J. 861 (1) (2018) 53, http://dx.doi.org/10.3847/1538-4357/aac6bf, arXiv:1708.01154.

[10] E. Di Valentino, S. Gariazzo, O. Mena, Most constraining cosmological neutrino mass bounds, Phys. Rev. D 104 (8) (2021) 083504, http://dx.doi.org/10.1103/PhysRevD.104.083504, arXiv:2106.15267.

[11] A. Aviles, A. Banerjee, G. Niz, Z. Slepian, Clustering in massive neutrino cosmologies via Eulerian perturbation theory, J. Cosmol. Astropart. Phys. 11 (2021) 028, http://dx.doi.org/10.1088/1475-7516/2021/11/028, arXiv:2106.13771.

[12] S. Wang, L. Hui, M. May, Z. Haiman, Is modified gravity required by observations? An empirical consistency test of dark energy models, Phys. Rev. D 76 (2007) 063503, http://dx.doi.org/10.1103/PhysRevD.76.063503, arXiv:0705.0165.

[13] E.J. Ruiz, D. Huterer, Testing the dark energy consistency with geometry and growth, Phys. Rev. D 91 (2015) 063009, http://dx.doi.org/10.1103/PhysRevD.91.063009, arXiv:1410.5832.

[14] J.L. Bernal, L. Verde, A.J. Cuesta, Parameter splitting in dark energy: is dark energy the same in the background and in the cosmic structures? J. Cosmol. Astropart. Phys. 02 (2016) 059, http://dx.doi.org/10.1088/1475-7516/2016/02/059, arXiv:1511.03049.

[15] J. Muir, et al., DES Collaboration, DES Y1 results: Splitting growth and geometry to test ΛCDM, Phys. Rev. D 103 (2) (2021) 023528, http://dx.doi.org/10.1103/PhysRevD.103.023528, arXiv:2010.05924.

[16] J. Ruiz-Zapatero, et al., Geometry versus growth - internal consistency of the flat ΛCDM model with KiDS-1000, Astron. Astrophys. 655 (2021) A11, http://dx.doi.org/10.1051/0004-6361/202141350, arXiv:2105.09545.

[17] U. Andrade, D. Anbajagane, R. von Marttens, D. Huterer, J. Alcaniz, A test of the standard cosmological model with geometry and growth, J. Cosmol. Astropart. Phys. 11 (2021) 014, http://dx.doi.org/10.1088/1475-7516/2021/11/014, arXiv:2107.07538.

[18] R.C. Bernardo, D. Grandón, J. Said Levi, V.H. Cárdenas, Parametric and nonparametric methods hint dark energy evolution, Phys. Dark Univ. 36 (2022) 101017, http://dx.doi.org/10.1016/j.dark.2022.101017, arXiv:2111.08289.

[19] F. Avila, A. Bernui, A. Bonilla, R.C. Nunes, Inferring $S_8(z)$ and $\gamma(z)$ with cosmic growth rate measurements using machine learning, 2022, arXiv:2201.07829.

[20] C. Rasmussen, C. Williams, Gaussian Processes for Machine Learning, in: Adaptive Computation and Machine Learning, MIT Press, Cambridge, MA, USA, 2006, p. 248.

[21] N. Aghanim, et al., Planck Collaboration, Planck 2018 results. VI. Cosmological parameters, Astron. Astrophys. 641 (2020) A6, http://dx.doi.org/10.1051/0004-6361/201833910, arXiv:1807.06209; Astron. Astrophys. 652 (2021) C4, Erratum.

[22] L. Perenon, M. Martinelli, S. Ilić, R. Maartens, M. Lochner, C. Clarkson, Multi-tasking the growth of cosmological structures, Phys. Dark Univ. 34 (2021) 100898, http://dx.doi.org/10.1016/j.dark.2021.100898, arXiv:2105.01613.

[23] G.F. Lesci, et al., AMICO galaxy clusters in kids-DR3: Cosmological constraints from counts and stacked weak lensing, Astron. Astrophys. 659 (2022) A88, http://dx.doi.org/10.1051/0004-6361/202040194, arXiv:2012.12273.

[24] T.M.C. Abbott, et al., DES Collaboration, Dark energy survey year 3 results: Cosmological constraints from galaxy clustering and weak lensing, Phys. Rev. D 105 (2) (2022) 023520, http://dx.doi.org/10.1103/PhysRevD.105.023520, arXiv:2105.13549.

[25] D. Kumar, D. Jain, S. Mahajan, A. Mukherjee, A. Rana, Constraints on the transition redshift using the cosmic triangle and hubble phase space portrait, 2022, arXiv:2205.13247.

[26] L. Kazantzidis, L. Perivolaropoulos, Evolution of the $f\sigma_8$ tension with the Planck15/ΛCDM determination and implications for modified gravity theories, Phys. Rev. D 97 (10) (2018) 103503, http://dx.doi.org/10.1103/PhysRevD.97.103503, arXiv:1803.01337.

[27] L. Kazantzidis, L. Perivolaropoulos, F. Skara, Constraining power of cosmological observables: blind redshift spots and optimal ranges, Phys. Rev. D 99 (6) (2019) 063537, http://dx.doi.org/10.1103/PhysRevD.99.063537, arXiv:1812.05356.

[28] L. Perenon, J. Bel, R. Maartens, A. de la Cruz-Dombriz, Optimising growth of structure constraints on modified gravity, J. Cosmol. Astropart. Phys. 06 (2019) 020, http://dx.doi.org/10.1088/1475-7516/2019/06/020, arXiv:1901.11063.

[29] D. Benisty, Quantifying the S_8 tension with the redshift space distortion data set, Phys. Dark Univ. 31 (2021) 100766, http://dx.doi.org/10.1016/j.dark.2020.100766, arXiv:2005.03751.

[30] C.J.A.P. Martins, M. Martinelli, E. Calabrese, M.P.L.P. Ramos, Real-time cosmography with redshift derivatives, Phys. Rev. D 94 (4) (2016) 043001, http://dx.doi.org/10.1103/PhysRevD.94.043001, arXiv:1606.07261.

[31] S. de la Torre, et al., The VIMOS public extragalactic redshift survey (VIPERS). Gravity test from the combination of redshift-space distortions and galaxy-galaxy lensing at $0.5 < z < 1.2$, Astron. Astrophys. 608 (2017) A44, http://dx.doi.org/10.1051/0004-6361/201630276, arXiv:1612.05647.

[32] F. Shi, et al., Mapping the real space distributions of galaxies in SDSS DR7: Ii. measuring the growth rate, clustering amplitude of matter and biases of galaxies at redshift 0.1, Astrophys. J. 861 (2) (2018) 137, http://dx.doi.org/10.3847/1538-4357/aacb20, arXiv:1712.04163.

[33] E. Jullo, et al., Testing gravity with galaxy-galaxy lensing and redshift-space distortions using CFHT-stripe 82, cfhtlens and BOSS CMASS datasets, Astron. Astrophys. 627 (2019) A137, http://dx.doi.org/10.1051/0004-6361/201834629, arXiv:1903.07160.

[34] H. Gil-Marín, W.J. Percival, L. Verde, J.R. Brownstein, C.-H. Chuang, F.-S. Kitaura, S.A. Rodríguez-Torres, M.D. Olmstead, The clustering of galaxies in the SDSS-III baryon oscillation spectroscopic survey: RSD measurement from the power spectrum and bispectrum of the DR12 BOSS galaxies, Mon. Not. R. Astron. Soc. 465 (2) (2017) 1757–1788, http://dx.doi.org/10.1093/mnras/stw2679, arXiv:1606.00439.

[35] M.M. Ivanov, O.H.E. Philcox, T. Nishimichi, M. Simonović, M. Takada, M. Zaldarriaga, Precision analysis of the redshift-space galaxy bispectrum, Phys. Rev. D 105 (6) (2022) 063512, http://dx.doi.org/10.1103/PhysRevD.105.063512, arXiv:2110.10161.

[36] O.H.E. Philcox, M.M. Ivanov, BOSS DR12 full-shape cosmology: ΛCDM constraints from the large-scale galaxy power spectrum and bispectrum monopole, Phys. Rev. D 105 (4) (2022) 043517, http://dx.doi.org/10.1103/PhysRevD.105.043517, arXiv:2112.04515.

[37] G. D'Amico, M. Lewandowski, L. Senatore, P. Zhang, Limits on primordial non-Gaussianities from BOSS galaxy-clustering data, 2022, arXiv:2201.11518.

[38] G. Cabass, M.M. Ivanov, O.H.E. Philcox, M. Simonović, M. Zaldarriaga, Constraints on multi-field inflation from the BOSS galaxy survey, 2022, arXiv:2204.01781.

[39] M. Chevallier, D. Polarski, Accelerating universes with scaling dark matter, Internat. J. Modern Phys. D 10 (2001) 213–224, http://dx.doi.org/10.1142/S0218271801000822, arXiv:gr-qc/0009008.

[40] E.V. Linder, Exploring the expansion history of the universe, Phys. Rev. Lett. 90 (2003) 091301, http://dx.doi.org/10.1103/PhysRevLett.90.091301, arXiv:astro-ph/0208512.

[41] O. Lahav, P.B. Lilje, J.R. Primack, M.J. Rees, Dynamical effects of the cosmological constant, Mon. Not. R. Astron. Soc. 251 (1991) 128–136.

[42] E.V. Linder, Cosmic growth history and expansion history, Phys. Rev. D 72 (2005) 043529, http://dx.doi.org/10.1103/PhysRevD.72.043529, arXiv:astro-ph/0507263.

[43] Z. Sakr, M. Martinelli, Cosmological constraints on sub-horizon scales modified gravity theories with MGCLASS II, J. Cosmol. Astropart. Phys. 05 (05) (2022) 030, http://dx.doi.org/10.1088/1475-7516/2022/05/030, arXiv:2112.14175.

[44] J. Ruiz-Zapatero, C. García-García, D. Alonso, P.G. Ferreira, R.D.P. Grumitt, Model-independent constraints on Ω_m and $H(z)$ from the link between geometry and growth, 2022, http://dx.doi.org/10.1093/mnras/stac431, arXiv:2201.07025.

[45] E. Ó Colgáin, M.M. Sheikh-Jabbari, Elucidating cosmological model dependence with H_0, Eur. Phys. J. C 81 (10) (2021) 892, http://dx.doi.org/10.1140/epjc/s10052-021-09708-2, arXiv:2101.08565.